MAPPING OF CERES BY DAWN: GENERATION OF HIGHER-LEVEL CARTOGRAPHIC PRODUCTS BASED ON FRAMING CAMERA DATA. A. Neesemann[1], S. van Gasselt[2], S.H.G. Walter[1], R. Jaumann[1], J.C. Castillo-Rogez[3], C.A. Raymond[3], C.T. Russell[4], F. Postberg[1]. [1]Freie Universität Berlin, Institute of Geological Sciences, Planetary Sciences and Remote Sensing. Malteserstr. 74-100, 12249 Berlin, Germany (a.neesemann@fu-berlin.de), [2]National Chengchi University, Department of Land Economics, Geomatics Group, No 64, Sec 2, ZhiNan Rd., Wenshan District, Taipei 11605, Taiwan, [3]Jet Propulsion Laboratory, California Institute of Technology, Pasadena, CA 91109, USA, [4]Institute of Geophysics and Planetary Physics, University of California, Pasadena, CA 91109, USA

Introduction: With the detection of subsurface oceans of liquid salty water under the icy crust of Europa [1,2] and Enceladus [3] (the latter also showing traces of organic compounds [4]), it became clear that the search for extraterrestrial life has to be expanded beyond the habitable zone. Recent discoveries made by the Dawn Science Team [5-12] show that Ceres shares a few commonalities with ocean worlds while also being much different. Without a considerable internal heat source or tidal heating keeping water liquid in large amounts, most of Ceres froze out, leaving behind a relict ocean world with a volatile-rich crust [13-16] and scattered subsurface brine reservoirs [9]. The most notable surface expressions of these brine reservoirs have been found within the fresh 92 km Occator crater in the form of a central cryovolcanic dome named Cerealia Tholus and its sorrounding bright deposits Cerealia Facula (CF) (Fig. 1) exposing carbonates [5, 6, 17] and ammonium chloride deposits [6], and several other dispersed thin bright deposits named Vinalia Faculae (VF) originating from rather explosive formation mechanisms [18]. Understandably, Occator crater is the taeget of a sample return mission [19, 20] to probe the evaporites evolved from the approximately 50 km deep brine reservoir beneath it [9, 12]. Planning and preparation of such a sample return mission requires the characterization of the potential landing site based on the most accurate topography and orthorectified image data. Here, we present the first two steps - the production of stereophotogrammetrically (SPG) and stereophotoclinometrically (SPC) derived digital terrain models (DTMs) and controlled, bundle-adjusted, photometrically corrected orthorectified image data and mosaics - necessary to produce matching Framing Camera (FC) [21] color cubes, slope maps and other higher-level data products such as pan-sharpened high resolution color data (Fig. 1), that constitute the base for processing the very high resolution data acquired during Dawn's final mission phase. Our entire workflow was implemented within the freely available USGS Integrated Software for Imagers and Spectrometers[1] (ISIS) and the Ames Stereo Pipeline[2] (ASP) [22] and will be made available for easy reproducibility.

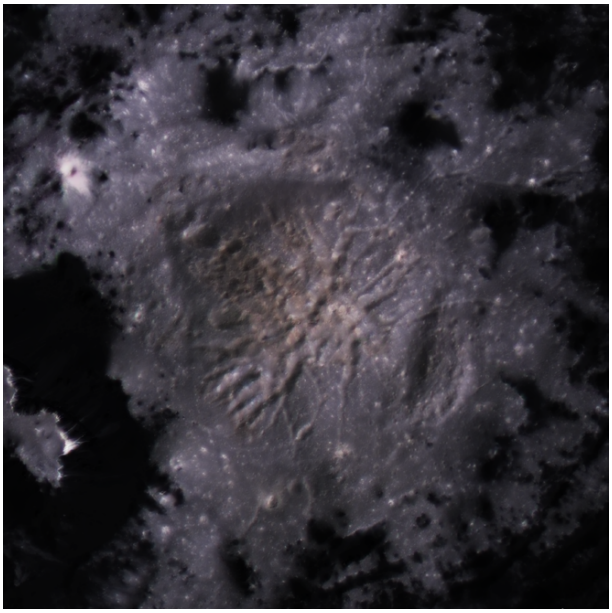

Fig. 1. Pan-sharpened, controlled hybrid mosaic compiled from bundle-adjusted panchromatic (F1) XM2-based images of the FC1 (5756-5757, 5921-5923, 5586-5587) and FC2 (92985-92987, 93153-93155, 93318-93320, 94735, 96325) and an RGB (F7, F2, F8) LAMO-based color composite.

Data and Methodology: We use images [21] of Ceres acquired during Dawn's nominal, 1st and especially 2nd extended mission (XM1 and XM2) at various altitudes (High Altitude Mapping Orbit (HAMO), Low Altitude Mapping Orbit (LAMO), and elliptical Extended Mission Orbit 7 (XMO7)). Complete coverage of Occator crater was achieved at a resolution of ~136 mpx^{-1} during the HAMO and XM1 Juling orbit by the panchromatic (F1) and the seven narrow band (F2-F8) filters and at ~34 mpx^{-1} during the LAMO and XM1 Extended LAMO by the F1. At ~34mpx^{-1}, filters F2-F8 also cover large areas of the crater, most importantly CF and VF, only leaving a 20-25 km wide NE-SW trending strip west of CF unmapped. Based on these data, global and local image mosaics [23-24] and SPG DTMs [25] and a global LAMO SPC DTM at 100 mpx^{-1} [26] were prepared and made available for public use via the PDS[3]. During Dawn's XM2, Occator was mainly mapped by the F1 at varying resolutions (2.7 to 40 mpx^{-1}) which requires an iterative approach to derive SPG and SPC DTMs for subsequent orthorectification and the production of seamless image mosaics. For the creation of data products presented here, we used the HAMO SPG DTM[3] [26] for the initial spice ingestion and co-registration of HAMO F1 image data. Subsequently, these bundle adjusted, photometrically corrected and map-projected F1 images were used to first create a HAMO-Juling SPG DTM and second the improved HAMO-Juling SPC DTM. The newly created HAMO-Juling SPC DTM and spacecraft position (SPK) and camera pointing (CK) SPICE kernels (and orthoimage mosaics) were then used to repeat the process for the higher resolved F1 LAMO data.

[1]https://isis.astrogeology.usgs.gov/
[2]https://ti.arc.nasa.gov/tech/asr/groups/intelligent-robotics/ngt/stereo/
[3]https://sbn.psi.edu/pds/resource/dawn/

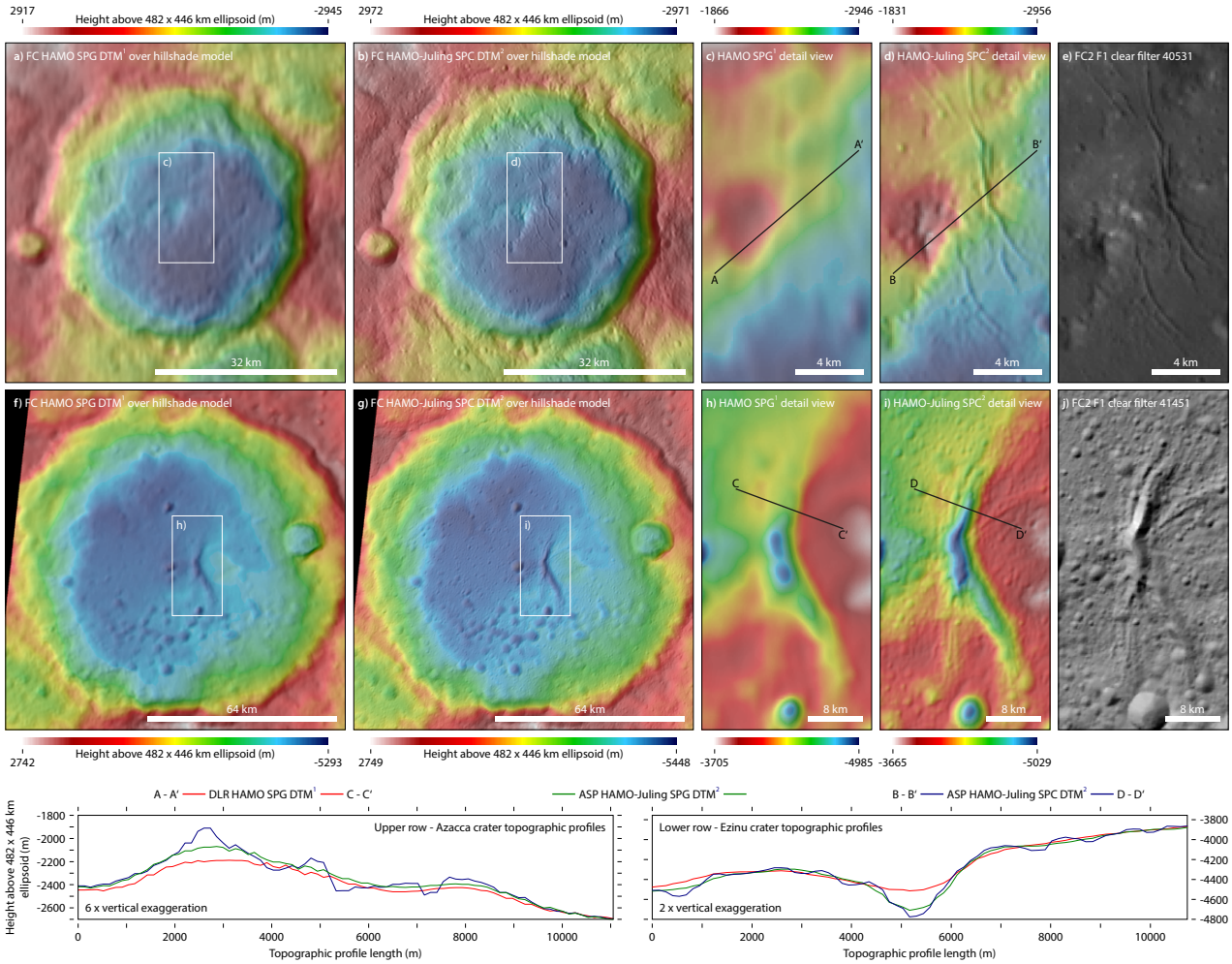

Fig. 2. Comparison between the DLR produced [1]HAMO-based SPG DTM [25], and our HAMO-Juling-based [2]SPG and [2]SPC DTMs. Upper row: Fresh 47 km in diamter *D* Azacca crater (6.71°S/218.34°E). Our HAMO-Juling-based SPC DTM resolves fine morphologic structures (central peak/grabens/cracks) that are otherwise not resolved in SPG-only DTMs. Lower row: Old 110 km in *D* Ezinu crater (42.95°N/195.19°W). The 4-5 km in *D* craters that form the E-W trending elongated cluster within Ezinu exibit sharp rim crests in the HAMO-Juing-based SPC DTM. Also, the 1-2 km wide v-shaped graben within Ezinu's center is resolved as such in the SPC DTM, while it rahter appears as a shallow bump in the SPG-only DTMs.

Results: We produced a regional HAMO-Juling and LAMO based SPG and SPC DTM ranging from 48°N-8°S and 196°E-284°E using all FC2 F1 images covering the above lat/lon range and corresponding orthoimage mosaics. Direct comparison between our HAMO-Juling SPG and the global HAMO SPG DTM [25] yields an average height difference of only 2.9 m. Larger differences mainly occur along steep slopes or in regions where our SPG DTM seems to have a slightly better resolution than the global HAMO SPG DTM [25] (as seen in the topographic profiles (bottom right in Fig. 2) of the central crack within Ezinu crater). In Fig. 2 we used the 47 km Azacca and 110 km Ezinu crater as examples to visualize the improvements achieved through SPC. Fine structures such as only a few px wide faults or craters that are resolved in the image data are also resolved in our SPC DTM, thus improving SPG DTMs by a factor of about 2-3. Based on our co-registered and bundle adjusted data, we derived new (SPK) and (CK) SPICE kernels that will be made available to allow interested users to create their own higher-level data products.

Acknowledgments: This work was partly supported by the German Aerospace Center (DLR) on behalf of the Federal Ministry of Economic Affairs and Energy, grant 50 OW 1101 and 50 OO 2204.

References: [1] Carr et al. 1998. *Nature* **391**. [2] Khurana et al. 2009. In: Pappalardo et al. (Eds.). *Europa.* University of Arizona Press, Tucson, 571-588. [3] Thomas et al. 2015. *Icarus* **264**. [4] Postberg et al. 2018. *Nature* **558**. [5] De Sanctis et al. 2020. *Space Sci. Rev.* **216**. [6] De Sanctis et al. 2020. *Nat. Astron.* **4**. [7] Nathues et al. 2020. *Nat. Astron.* **4**, 794-801. [8] Park et al. 2020. *Nat. Astron.* **4**, 748-755. [9] Raymond et al. 2020. *Nat. Astron.* **4**. [10] Schenk et al. 2020. *Nat. Commun.* **11**. [11] Schmidt et al. 2020 *Nat. Geosci.* **13**. [12] Scully et al. 2020. *Nat. Commun.* **11**. [13] Park et al. 2016. *Nature* **537**. [14] Ermakov et al. 2017. *JGR* **122**. [15] Konopliv et al. 2018. *Icarus* **299**. [16] Prettyman et al. 2021. *GRL* **48**. [17] De Sanctis et al. 2016. *Nature* **536**. [18] Ruesch et al. 2019. *Icarus* **320**. [19] Gassot et al. 2021. *Acta Astronaut.* **181**. [20] Scully et al. 2021. *Planet. Sci. J.* **2**. [21] Sierks et al. 2011. *Space Sci. Rev.* **163**. [22] Beyer et al. 2018. *Earth Space Sci.* **5**. [23] Roatsch et al. 2016. *Planet. Space Sci.* **129**. [24] Roatsch et al. 2017. *Planet. Space Sci.* **140**. [25] Preusker et al. 2016. 47th *LPSC* (abs. 1954). [26] Park et al. 2019. *Icarus* **319**.